Cellular and Molecular Life Sciences (2020) 77:2997–3012
https://doi.org/10.1007/s00018-019-03322-y

ORIGINAL ARTICLE

CFP1-dependent histone H3K4 trimethylation in murine oocytes facilitates ovarian follicle recruitment and ovulation in a cell-nonautonomous manner

Qian-Qian Sha[1,2] · Yu Jiang[1] · Chao Yu[1] · Yunlong Xiang[3] · Xing-Xing Dai[1] · Jun-Chao Jiang[1] · Xiang-Hong Ou[2] · Heng-Yu Fan[1]

Received: 2 May 2019 / Revised: 22 September 2019 / Accepted: 25 September 2019 / Published online: 1 November 2019

Abstract

CxxC-finger protein 1 (CFP1)-mediated trimethylated histone H3 at lysine-4 (H3K4me3) during oocyte development enables the oocyte genome to establish the competence to generate a new organism. Nevertheless, it remains unclear to which extent this epigenetic modification forms an instructive component of ovarian follicle development. We investigated the ovarian functions using an oocyte-specific *Cxxc1* knockout mouse model, in which the H3K4me3 accumulation is downregulated in oocytes of developing follicles. CFP1-dependent H3K4 trimethylation in oocytes was necessary to maintain the expression of key paracrine factors and to facilitate the communication between an oocyte and the surrounding granulosa cells. The distinct gene expression patterns in cumulus cells within preovulatory follicles were disrupted by the *Cxxc1* deletion in oocytes. Both follicle growth and ovulation were compromised after CFP1 deletion, because *Cxxc1* deletion in oocytes indirectly impaired essential signaling pathways in granulosa cells that mediate the functions of follicle-stimulating hormone and luteinizing hormone. Therefore, CFP1-regulated epigenetic modification of the oocyte genome influences the responses of ovarian follicles to gonadotropin in a cell-nonautonomous manner.

Keywords CxxC-finger protein 1 · Histone H3K4 trimethylation · Oocyte · Follicle development · Ovulation · Cumulus cell expansion

Introduction

Follicles are functional units of the mammalian ovary, and each follicle consists of an oocyte surrounded by one or more layers of somatic cells. A neonatal ovary is endowed with several million primordial follicles, consisting of an oocyte surrounded by a single layer of flattened pregranulosa cells [1]. Of those dormant primordial follicles that survive and are recruited into the growing follicle population, very few are destined to ovulate; the majority will degenerate at some point along this lengthy developmental continuum (duration of weeks in rodents to months in humans) [28].

Progression of follicle development requires bidirectional communication between an oocyte and granulosa cells (GCs). Later stages of follicle development, including the process of follicle selection and ovulation, are also dependent on appropriately timed endocrine signals, notably, pituitary gonadotropins and a myriad of locally produced factors operating in an autocrine or paracrine manner to coordinate and control ovarian function [11]. Three growth factors,

Electronic supplementary material The online version of this article (https://doi.org/10.1007/s00018-019-03322-y) contains supplementary material, which is available to authorized users.

✉ Xiang-Hong Ou
ouxh@gd2h.org.cn

✉ Heng-Yu Fan
hyfan@zju.edu.cn

[1] Life Sciences Institute, Zhejiang University, 866 Yuhangtang Rd, Hangzhou 310058, China

[2] Fertility Preservation Laboratory, Reproductive Medicine Center, Guangdong Second Provincial General Hospital, Guangzhou 510317, China

[3] Center for Stem Cell Biology and Regenerative Medicine, MOE Key Laboratory of Bioinformatics, THU-PKU Center for Life Sciences, School of Life Sciences, Tsinghua University, Beijing 100084, China

growth differentiation factor 9 (GDF9), bone morphogenetic protein 15 (BMP15), and fibroblast growth factor 8 (FGF8), are expressed in an oocyte-specific manner and play key roles in promoting follicle growth beyond the primary stage [10, 29, 40]. Furthermore, they determine the differentiation of cumulus cells and their responses to ovulation signals in preovulatory follicles [20, 39]. Therefore, they are also called oocyte-derived cumulus expansion-enabling factors [12, 42].

On the other hand, the accumulation and resetting of epigenetic marks during oocyte development enables the oocyte genome to establish the competence to generate a new organism [16, 46, 48]. Despite extensive mapping of oocyte chromatin patterns, the extent to which histone modifications form an instructive component of ovarian follicle development remains unclear. A hallmark of active chromatin is trimethylated H3 at lysine-4 (H3K4me3), which is enriched in active promoters and correlates with transcriptional activity [3, 6, 35]. Recent reports revealed deposition of broad domains of H3K4me3 in mature oocytes, predominantly in partially methylated regions [25, 46]. Mixed-lineage leukemia 2 (MLL2) and SET domain-containing 1 (SETD1)-Cxxc finger protein 1 (CFP1) histone methyltransferases are reported to confer this unusual distribution of H3K4me3 as well as the developmental competence onto mouse oocytes [2, 44]. Nevertheless, whether H3K4me3 contributes to oocytes' capacity for facilitating follicle recruitment and ovulation in estrus cycles remains unexplored.

To address these outstanding questions, we took advantage of an oocyte-specific *Cxxc1* knockout mouse model where H3K4 trimethylation is selectively ablated in oocytes of developing follicles [44]. Employing multiple experimental approaches, we demonstrated that the CFP1 deletion in growing oocytes impaired both follicle growth and ovulation in response to gonadotropin stimulations. CFP1-mediated histone H3 lysine-4 trimethylation in an oocyte was necessary to maintain the normal expression of key paracrine factors which facilitate the communication between an oocyte and the surrounding GCs. Therefore, the posttranslational histone modification of the oocyte genome not only gives developmental competence to a zygote after fertilization as demonstrated in previous studies, but also maintains the appropriate responses of ovarian somatic cells to gonadotropin in a cell-nonautonomous manner.

Results

Cxxc1 deletion in mouse oocytes decreases transcription activity in growing follicles

We have reported selective deletion of *Cxxc1* in growing oocytes via crossing of *Cxxc1*$^{fl/fl}$ mice with *Zp3-Cre* mice [44]. In this study, we knocked out *Cxxc1* in oocytes as early as the primordial follicle stage, using the well-characterized *Gdf9-Cre* (*Cxxc1*$^{fl/fl}$*;Gdf9-Cre*, later termed as *Cxxc1*$^{oo-/-}$). The strategy of developmental stage-specific *Cxxc1* knockout is illustrated in Fig. 1a. As previously reported, both *Cxxc1*$^{fl/fl}$*;Gdf9-Cre* and *Cxxc1*$^{fl/fl}$*;Zp3-Cre* females were completely infertile [34, 44]. Efficient deletion of CFP1 protein in the oocyte of *Cxxc1*$^{oo-/-}$ mice at postnatal day (PD) 21 was confirmed by western blotting (Fig. 1b) and immunofluorescent staining on ovarian sections (Fig. 1c, arrows indicate oocytes). Nonetheless, the expression level of CFP1 in the surrounding granulosa cells was not affected by *Cxxc1*-deletion in the oocytes (Fig. 1c). It was shown that knockout of *Mll2*, another H3K4 methyltransferase, in mouse oocytes impairs H3K4me3 accumulation and caused defects of oocyte development [17]. Therefore, we compared the levels of mRNAs encoding *Setd1a*, *Setd1b*, *Cxxc1*, and *Mll2*, by quantitative RT-PCR in fully grown oocytes. The amplification efficiencies of each pair of PCR primers were normalized. The results demonstrated that the expression levels of *Cxxc1* transcripts were more abundant than that of *Mll2* transcripts in oocytes (Fig. 1d). Importantly, the expression of *Setd1a*, *Setd1b*, and *Mll2* mRNAs was not significantly affected in *Cxxc1*-deleted oocytes (Fig. 1e). In addition, we detected an increase of MLL2 protein level in *Cxxc1* null oocytes, probably due to a feedback mechanism trying to compensate the loss of CFP1 (Fig. 1b).

In the ovaries of wild-type (WT) mice on PD21, the H3K4me3 level in oocytes of primordial follicles (indicated by arrows) was comparable to that in the surrounding somatic cells, but gradually increased in oocytes during follicle growth, particularly at secondary and antral follicle stages (Fig. 2a, c). In comparison, H3K4me3 failed to accumulate in *Cxxc1*-null oocytes of growing follicles. The H3K4me3 level in GCs remained stable during follicle development and was not affected by the *Cxxc1* knockout in oocytes (Fig. 2a). In WT oocytes, the phosphorylation level of RNA polymerase II (pS2, which reflects global transcriptional activity) was high in oocytes at the secondary follicle stage, but decreased at the antral follicle stage. On the other hand, the pS2 level was significantly lower than normal in *Cxxc1*-null oocytes at these stages (Fig. 2b, d).

Both RNA sequencing and quantitative RT-PCR results showed that genes encoding oocyte-specific paracrine factors, including *Gdf9*, *Bmp15*, *Fgf8*, *c-Kit*, and *Oosp1*, were significantly downregulated in *Cxxc1*-null oocytes at PD21 (Fig. 2e, f). So was *Gja4*, which encodes a connexin-37 subunit crucial for oocyte–GC communication [33, 37]. To further verify whether oocyte-specific paracrine factors are regulated by H3K4me3 levels, we performed chromatin immunoprecipitation (ChIP)-qPCR assays using 300 GV oocytes to investigate the levels of H3K4me3 on the promoter regions of *Gdf9*, *Bmp15*, *Fgf8*, *c-Kit*, *Oosp1,* and

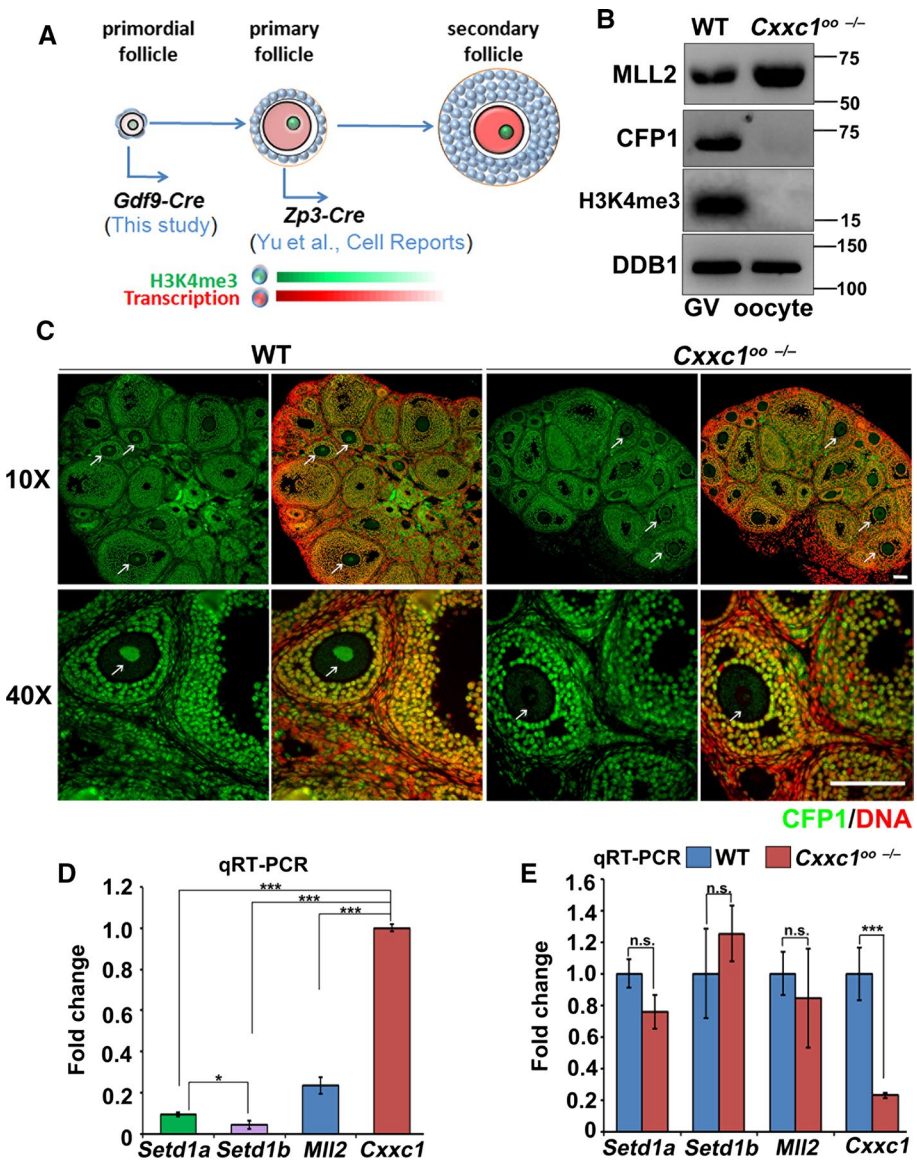

Fig. 1 Expression of SETD1-CFP1 and MLL2 in *Cxxc1*-deleted oocytes. **a** The strategy of developmental stage-specific *Cxxc1* knockout in mouse oocytes. **b** Western blotting results showing the protein levels of MLL2, CFP1, and H3K4me3 in fully grown GV oocytes collected from WT and $Cxxc1^{oo-/-}$ mice. Endogenous DDB1 was used as a loading control. Total proteins from 100 oocytes were loaded in each lane. **c** Immunofluorescence results showing the levels of CFP1 in the oocytes and GCs of WT and $Cxxc1^{oo-/-}$ mice at postnatal day (PD) 21. Arrows indicate oocytes. Scale bar 50 μm. Six ovaries from three females for each genotype were analyzed. **d** Quantitative RT-PCR results showing expression levels of mRNAs encoding *Setd1a*, *Setd1b*, *Mll2*, and *Cxxc1* in fully grown GV oocytes. The expression level of *Cxxc1* was set as 1, and levels of other transcripts were normalized accordingly. **e** Quantitative RT-PCR results showing expression levels of mRNAs encoding *Setd1a*, *Setd1b*, *Mll2*, and *Cxxc1* in fully grown GV oocytes of WT and $Cxxc1^{oo-/-}$ mice. The expression level of each transcript in WT oocytes was set as 1. Error bars: SEM. $^{***}P < 0.001$ according to two-tailed Student's *t* test; *n.s.* nonsignificant

Gja4. The results showed that the H3K4me3 levels on the promoters of these genes in *Cxxc1*-null oocytes were significantly lower than those in WT oocytes (Fig. 2g). These results indicate that the downregulation of these genes was caused by the effect of the SETD1–CFP1 complex on transcription-coupled H3K4 trimethylation at the promoter regions.

Follicle growth is impaired by the *Cxxc1* knockout in oocytes

At PD28, which is the stage where female mice undergo the transition from puberty to sexual maturation, the ovaries of $Cxxc1^{oo-/-}$ mice were already smaller than those of their control litter mates (Fig. 3a, b). Six-month-old adult $Cxxc1^{oo-/-}$ females also had smaller ovaries than did WT mice of the same age (Fig. 3a, b). Because our previous study has already proved that the *Cxxc1* knockout does not affect the survival of primordial follicles [44], we hypothesized that CFP1 in oocytes might be necessary to support follicle development beyond this stage.

Ovarian histological analyses at PD28 indicated that the numbers of primordial and primary follicles were similar between WT and $Cxxc1^{oo-/-}$ mice, suggesting that the primordial follicle formation and activation processes were not affected by the *Cxxc1* deletion in oocytes (Fig. 3c, d). Nevertheless, there were much fewer early secondary follicles (which contain 2–3 layers of GCs) and antral follicles (characterized by the presence of an antral cavity) in the $Cxxc1^{oo-/-}$ ovaries than in normal ones (Fig. 3c, d). The numbers of late secondary follicles that contain more than three layers of GCs also moderately decreased

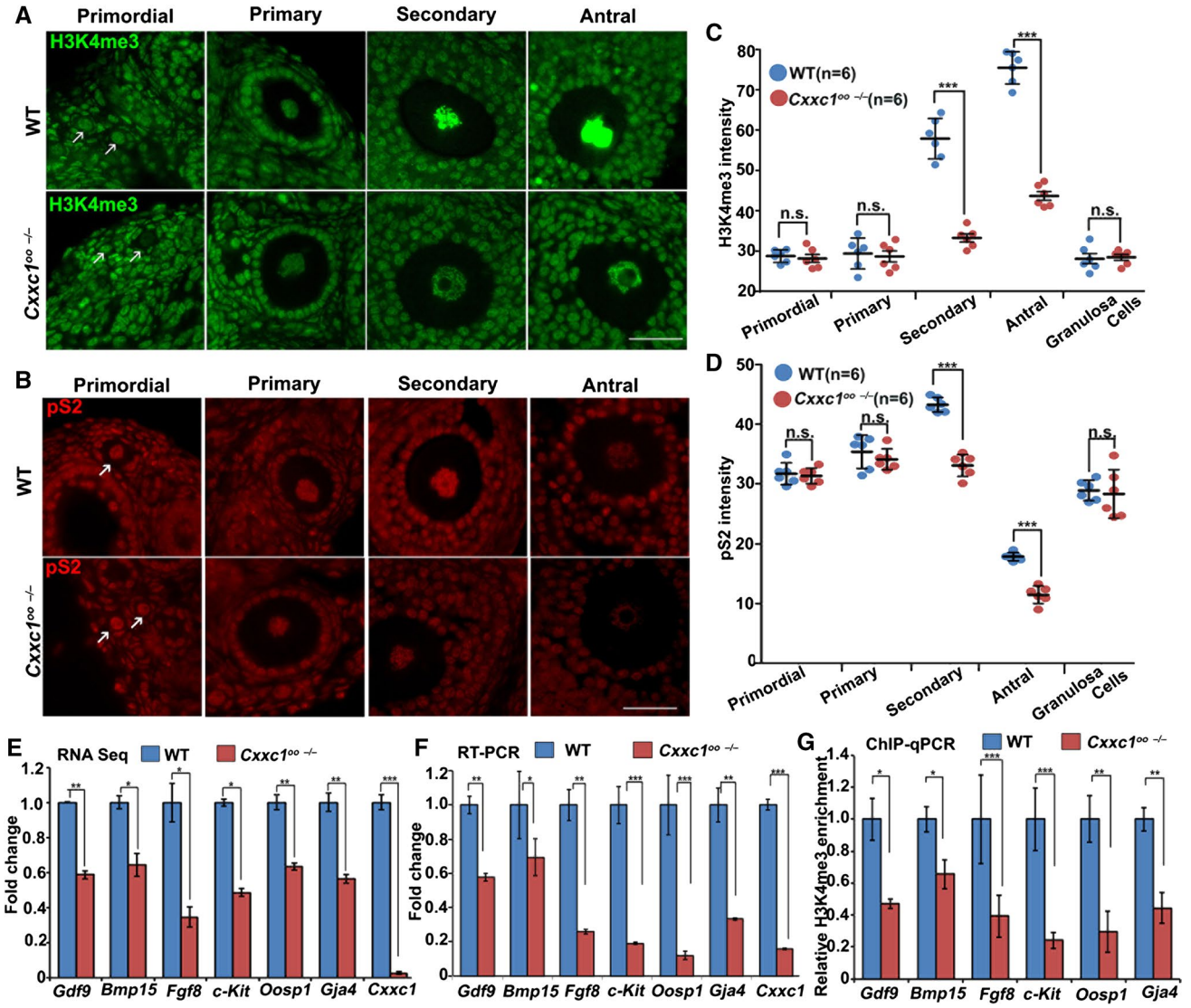

Fig. 2 Changes of gene expression and histone H3 trimethylation in *Cxxc1* knockout oocytes. Immunofluorescence results showing the levels of H3K4me3 (**a**) and phosphorylated RNA polymerase II CTD repeat YSPTSPS (pS2) (**b**) in the oocytes and GCs of WT and *Cxxc1*$^{oo-/-}$ mice. The stages of follicles are specified. Arrows indicate oocytes within primordial follicles. Scale bar 50 μm. Six ovaries from three females for each genotype were analyzed. **c**, **d** Quantification of H3K4me3 and pS2 signals in **a**, **b**, respectively. Error bars: SEM. ***$P<0.001$ according to two-tailed Student's *t* test; *n.s.* nonsignificant. Relative expression of selected genes extracted from RNA-seq data (**e**) and determined by qRT-PCR (**f**). Error bars: SEM. ***$P<0.001$, **$P<0.01$, and *$P<0.05$ according to two-tailed Student's *t* test. **g** ChIP-qPCR analysis of H3K4me3 levels on the promoter regions of indicated genes. All enrichment values are relative to input values and then normalized with enrichment values of WT samples. Error bars: SEM. ***$P<0.001$, **$P<0.01$, and *$P<0.05$ according to two-tailed Student's *t* test

in *Cxxc1*$^{oo-/-}$ ovaries but not as significantly as in the early secondary follicles and antral follicles. A likely explanation for this phenomenon is that the transition from the secondary to antral follicle stage was impaired in *Cxxc1*$^{oo-/-}$ ovaries and, therefore, caused relative accumulation of late secondary follicles. Follicles and corpus lutea (CL) at various developmental stages were also present on ovarian sections of 6-month-old *Cxxc1*$^{oo-/-}$ mice (Fig. 3e). Similar to the results of follicle counts at 4 weeks old, the number of secondary follicles, but not primordial and primary follicles, decreased in the ovary of 6-month-old *Cxxc1*$^{oo-/-}$ mice, but the numbers of primary follicles were not affected (Fig. 3f). These results further indicated that *Cxxc1* deletion in oocytes caused follicle growth retardation instead of premature ovarian failure.

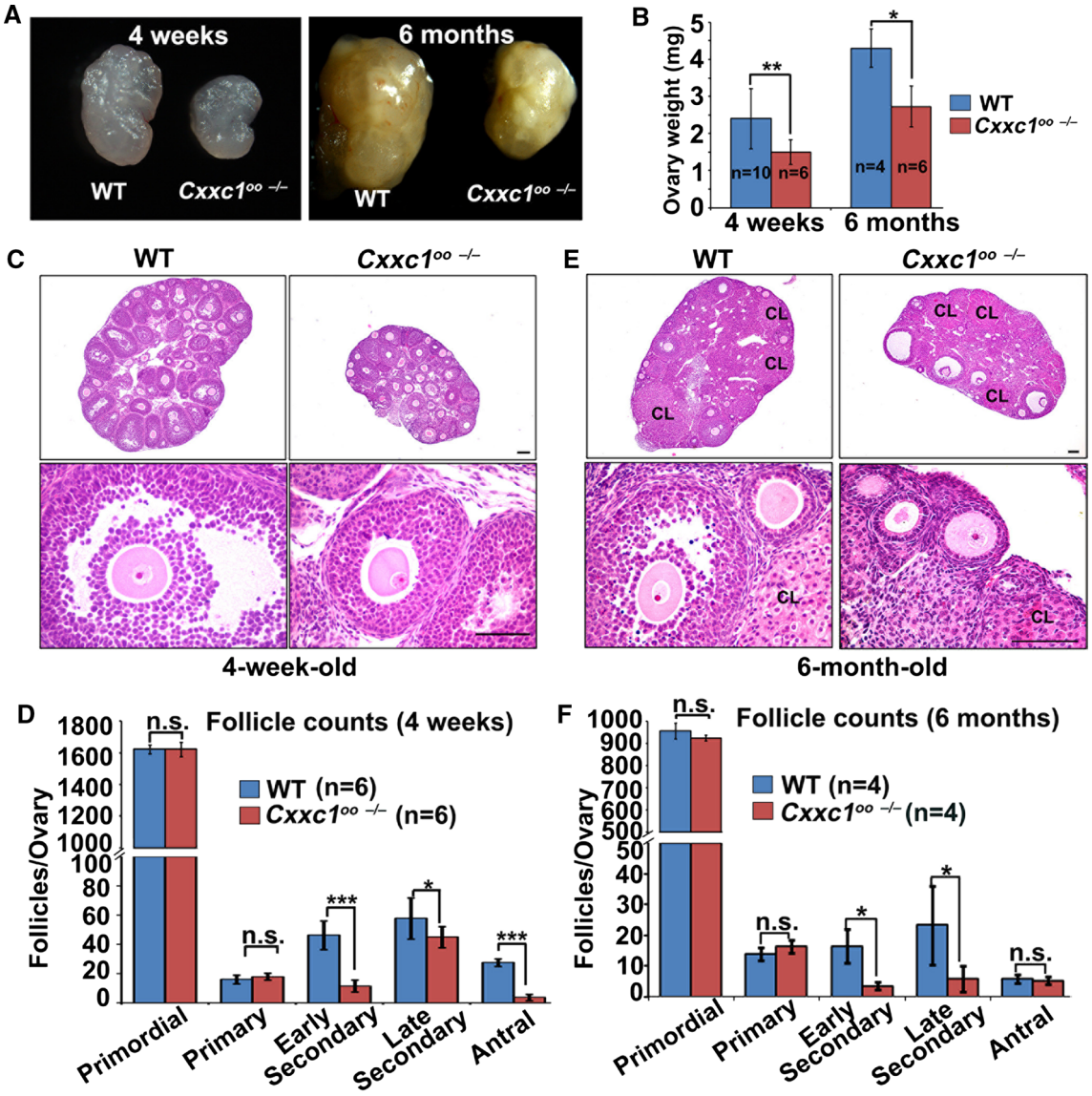

Fig. 3 Follicle development in the ovaries of *Cxxc1*$^{oo-/-}$ mice. Size (**a**) and weight (**b**) comparisons between WT and *Cxxc1*$^{oo-/-}$ ovaries at 4 weeks and 6 months; n: the number of ovaries analyzed for each genotype. Error bars: SEM; $0.01 < {}^{*}P < 0.05$ according to two-tailed Student's *t* test. Scale bar 500 µm. **c**, **e** H&E staining results showing ovarian histology of 4-week-old and 6-month-old WT and *Cxxc1*$^{oo-/-}$ mice. Scale bar 100 µm. Serial follicle counts in ovaries of 4-week-old (**d**) and 6-month-old (**f**) WT and *Cxxc1*$^{oo-/-}$ mice. Six ovaries from different females for each genotype were analyzed. Error bars: SEM. $^{***}P < 0.001$, $^{**}P < 0.01$, and $^{*}P < 0.05$ according to two-tailed Student's *t* test; *n.s.* nonsignificant

GC proliferation and apoptosis were affected by the *Cxxc1* knockout in oocytes

At PD28, increased GC apoptosis and follicle atresia were detected by immunohistochemical staining of cleaved caspase 3 (CC3) and a TdT-mediated dUTP Nick-End Labeling (TUNEL) assay in the ovaries of *Cxxc1*$^{oo-/-}$ mice in contrast to the ovaries of control mice (Fig. 4a). Quantifying atretic follicles versus total follicles on ovarian sections indicated that the ovaries of *Cxxc1*$^{oo-/-}$ mice had greater numbers of atretic follicles (Fig. 4b). On the contrary, fewer dividing GCs labeled with the mitotic cell marker phosphorylated histone H3 at serine-10 were detected in the growing follicles of *Cxxc1*$^{oo-/-}$ mice than in those of control mice (Fig. 4c, d).

FSH receptor (encoded by *Fshr* gene) expressed by GCs is essential for follicle growth beyond the early antral follicle stage [9]. Expression of *Fshr* was not statistically affected by the *Cxxc1* knockout in oocytes (Fig. 4e). Because FSH stimulates follicle growth and prevents atresia by elevating phosphoinositide 3-kinase (PI3K) pathway activity [13, 23], we evaluated the amounts of phosphorylated AKT and ribosome protein S6 (pRPS6)

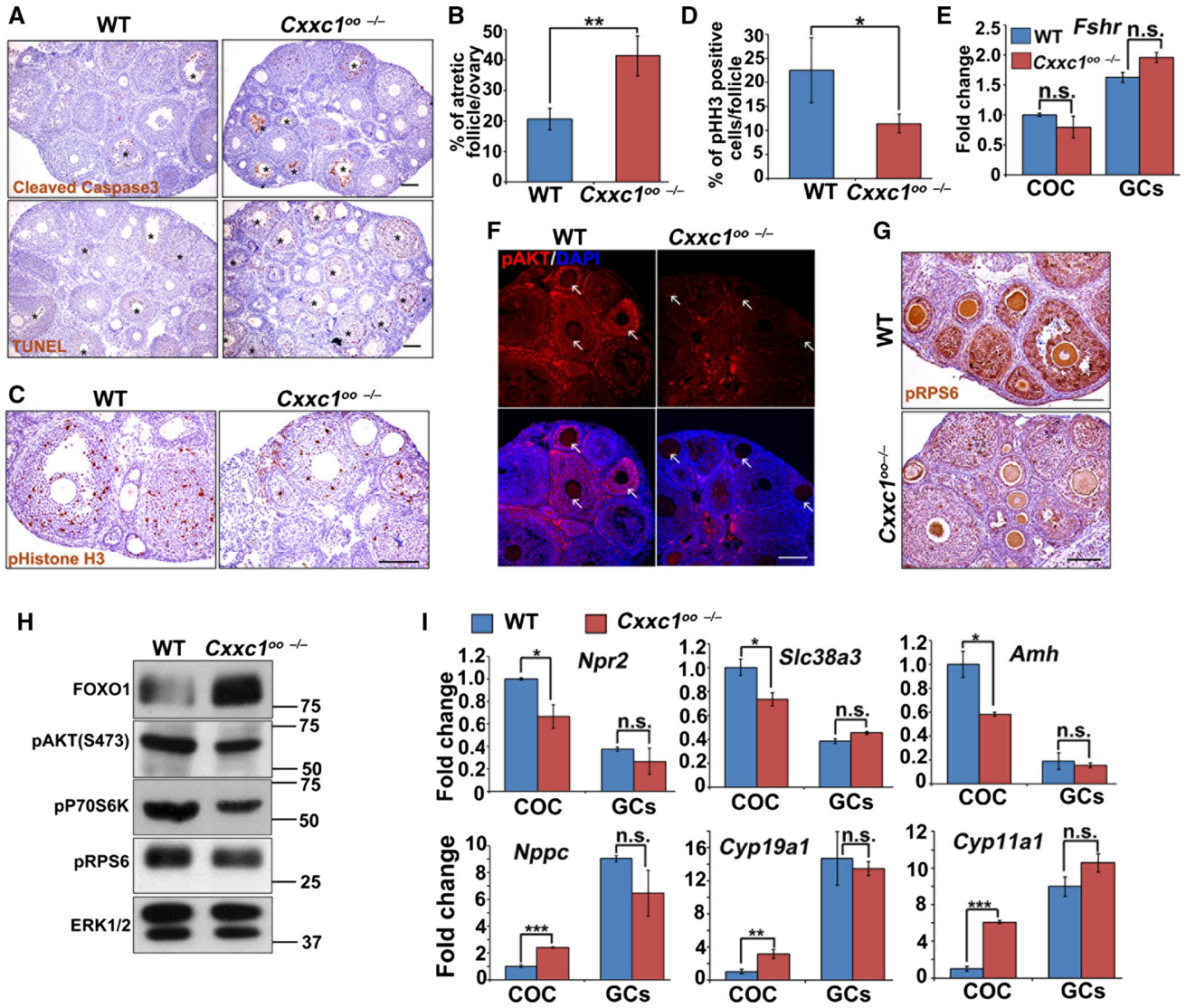

Fig. 4 Impaired signaling pathways and gene expression patterns in the developing follicles of *Cxxc1*$^{oo-/-}$ mice. **a** Immunohistochemical data on cleaved caspase 3 and TUNEL assay show an increase in GC apoptosis and follicle atresia in 4-week-old *Cxxc1*$^{oo-/-}$ ovaries as compared with WT. Scale bar 100 μm. Asterisks indicate atretic follicles. **b** Quantification of TUNEL-positive atretic follicles in 4-week-old WT and *Cxxc1*$^{oo-/-}$ ovaries. Error bars: SEM. $^{**}P<0.01$ according to two-tailed Student's *t* test. Immunohistochemical (**c**) and quantification (**d**) results for phospho-histone H3 (pH3-Ser10) indicating GC proliferation in 4-week-old WT and *Cxxc1*$^{oo-/-}$ ovaries. Scale bar 100 μm. Error bars: SEM. $^{*}P<0.05$ according to two-tailed Student's *t* test. **e** Quantitative RT-PCR results for the expression levels of FSH receptor (*Fshr*) mRNA in GCs and COCs isolated from 4-week-old WT and *Cxxc1*$^{oo-/-}$ ovaries. Error bars: SEM; *n.s.* nonsignificant. **f** Immunofluorescence results on p-AKT(Ser 473) in 4-week-old WT and *Cxxc1*$^{oo-/-}$ ovaries. Arrows indicate oocytes within activated follicles. Scale bar 100 μm. Arrows indicate growing follicles. **g** Immunohistochemical results on p-RPS6 (Ser235/236) in 4-week-old WT and *Cxxc1*$^{oo-/-}$ ovaries. Scale bar 100 μm. **h** Western blot analysis of PI3K pathway components, including FOXO1, p-AKT (Ser 473), and p-RPS6 (Ser235/236) in 4-week-old WT and *Cxxc1*$^{oo-/-}$ ovaries. ERK1 and -2 served as a loading control. Total-protein samples were extracted from four ovaries in each group, and 30 μg of total protein was loaded per lane; each experiment was repeated at least three times. **i** Quantitative RT-PCR results on mRNA levels of genes specifically expressed in COCs (*Npr2*, *Slc38a3*, and *Amh*) and genes more expressed in GCs (*Nppc*, *Cyp19a1*, and *Cyp11a1*) from WT and *Cxxc1*$^{oo-/-}$ ovaries at 44 h after PMSG injection. Error bars: SEM. $^{**}P<0.01$ and $^{*}P<0.05$ according to two-tailed Student's *t* test; *n.s.* nonsignificant

in the ovaries of WT and *Cxxc1*$^{oo-/-}$ mice by immunofluorescent and immunohistochemical analyses, respectively. AKT is a key component of the PI3K pathway and a multifunctional kinase. Its general function is to inhibit apoptosis and to stimulate cell proliferation [5]. Besides, activated AKT increases the cellular protein synthesis rate by inducing sequential phosphorylation of its downstream proteins P70 ribosome protein S6 kinase (P70RSK) and ribosome protein S6 (RPS6) [32]. The growing follicles of *Cxxc1*$^{oo-/-}$ mice had significantly

lower p-AKT and pRPS6 levels compared with those in control mice (Fig. 4f, g). The reduced activity of the PI3K signaling pathway was next verified by western blot analyses of GCs isolated from the ovaries of 4-week-old WT and *Cxxc1*$^{oo-/-}$ mice (Fig. 4h). Amounts of phosphorylated AKT, P70RSK, and RPS6 all decreased in GCs from *Cxxc1*$^{oo-/-}$ mice. In addition, transcriptional repressor forkhead box O1 (FOXO1) is highly expressed in GCs of slowly growing follicles. It represses GC proliferation and steroidogenesis and facilitates follicle atresia. Normally, an activated PI3K pathway releases follicles from this inhibitory state by triggering phosphorylation and degradation of FOXO1 [27]. Our western blot results indicated that the protein levels of FOXO1 were significantly higher in GCs of *Cxxc1*$^{oo-/-}$ ovaries (Fig. 4h). Collectively, these results suggested that the *Cxxc1* deletion in oocytes indirectly impaired PI3K signaling in the surrounding GCs and facilitated follicle atresia.

CFP1 in an oocyte is required for maintaining a specific gene expression pattern in cumulus cells

Cumulus cells, which are closely associated with an oocyte, promote oocyte growth and developmental competence through complex bidirectional interactions with the oocyte. Influenced by concentration gradients of oocyte-secreted factors, mural and cumulus cells each express a subset of different transcripts [8]. The C-type natriuretic peptide–natriuretic peptide receptor 2 (NPR2) signaling pathway is essential for maintaining high cGMP levels in cumulus–oocyte complexes (COCs) and for preventing precocious germinal vesicle breakdown (GVBD) [47]. *Nppc* is a gene that encodes secreted factor C-type natriuretic peptide and is highly expressed in mural GCs. In contrast, the gene of its receptor, *Npr2*, is more prominently expressed in cumulus cells than in mural GCs (Fig. 4i). This result is in agreed with the reported observation [47]. In the COCs of PMSG-primed *Cxxc1*$^{oo-/-}$ mice, the mRNA levels of *Npr2* and *Nppc* were dramatically lower and higher as compared with WT controls, respectively (Fig. 4i). Similarly, other genes that are preferentially expressed by COCs rather than GCs, e.g., *Slc38a3* and *Amh*, were downregulated after the *Cxxc1* knockout in oocytes. By contrast, the genes that normally have a lower expression level in COCs than in GCs, including *Cyp19a1* and *Cyp11a1*, were upregulated in COCs of *Cxxc1*$^{oo-/-}$ mice. Overall, the expression levels of these genes in GCs were not significantly affected by the *Cxxc1* knockout in oocytes. Collectively, these results indicated that the distinct gene expression patterns in cumulus cells within preovulatory follicles were disrupted by *Cxxc1* deletion in oocytes.

The in vitro growth defect of *Cxxc1*$^{oo-/-}$ follicles can be partially rescuing by the PI3K activator 740Y-P

It has been reported that artificial activation of PI3K pathway in the mouse and human ovaries was able to stimulate follicle growth [41]. Therefore, we cultured secondary follicles isolated from *Cxxc1*$^{oo-/-}$ mice in medium-containing a PI3K activator 740Y-P (100 μg/ml). This treatment had a rescuing effect and increased the rate of *Cxxc1*$^{oo-/-}$ follicles that developed to the antral stage (Fig. 5a, b). We also investigated if PI3K pathway in the GCs of *Cxxc1*$^{oo-/-}$ follicles was indeed activated by 740Y-P treatment. Western blot results showed that PI3K pathway components including AKT, P70S6K and RPS6 were all phosphorylated after 740Y-P treatment, in GCs from both WT and *Cxxc1*$^{oo-/-}$ mice (Fig. 5c). Furthermore, we isolated COCs from cultured WT and *Cxxc1*$^{oo-/-}$ follicles (with or without 740Y-P treatment) and further cultured with or without EGF, a stimulator of cumulus cell expansion. Compact COCs with multiple layers of cumulus cells could be isolated from WT follicles after culture, and these COCs underwent expansion after EGF treatment (Fig. 5d). However, COCs isolated from *Cxxc1*$^{oo-/-}$ follicles contained less cumulus cells which frequently dissociated from the oocytes after culture. The presence of 740Y-P in medium improved the morphology of the COCs as well as their in vitro expansion responses to EGF (Fig. 5d).

CFP1 in oocytes regulates GC function during ovulation by a cell-nonautonomous mechanism

Although the follicles containing *Cxxc1*-null oocytes have a low growth rate under natural conditions, the first wave of follicle development to the preantral stage was normal in the ovaries of 3-week-old *Cxxc1*$^{oo-/-}$ mice. PMSG injection at PD21–23 stimulated the formation of comparable numbers of large antral stage follicles in the ovaries of *Cxxc1*$^{oo-/-}$ mice (Fig. 6a, b). Nonetheless, subsequent hCG injection failed to induce effective meiotic resumption (characterized by GVBD, Fig. 6c) and ovulation (Fig. 6d) in these mice. At 8 h after hCG injection, ovaries of *Cxxc1*$^{oo-/-}$ mice were much smaller than the control ovaries, indicating a poor response to gonadotropins (Fig. 6e). Cumulus expansion was significantly impaired in the preovulatory follicles of *Cxxc1*$^{oo-/-}$ mice when compared with that in WT mice (Fig. 6f). Subsequently, preovulatory follicles did not rupture at 16 h after hCG injection (Fig. 6g). In an in vitro cumulus expansion assay, EGF mimicked the function of EGF-like factors and induced expansion of cultured COCs isolated from WT mice. In contrast, COCs collected from *Cxxc1*$^{oo-/-}$ mice were nonresponsive to the EGF treatment (Fig. 6h).

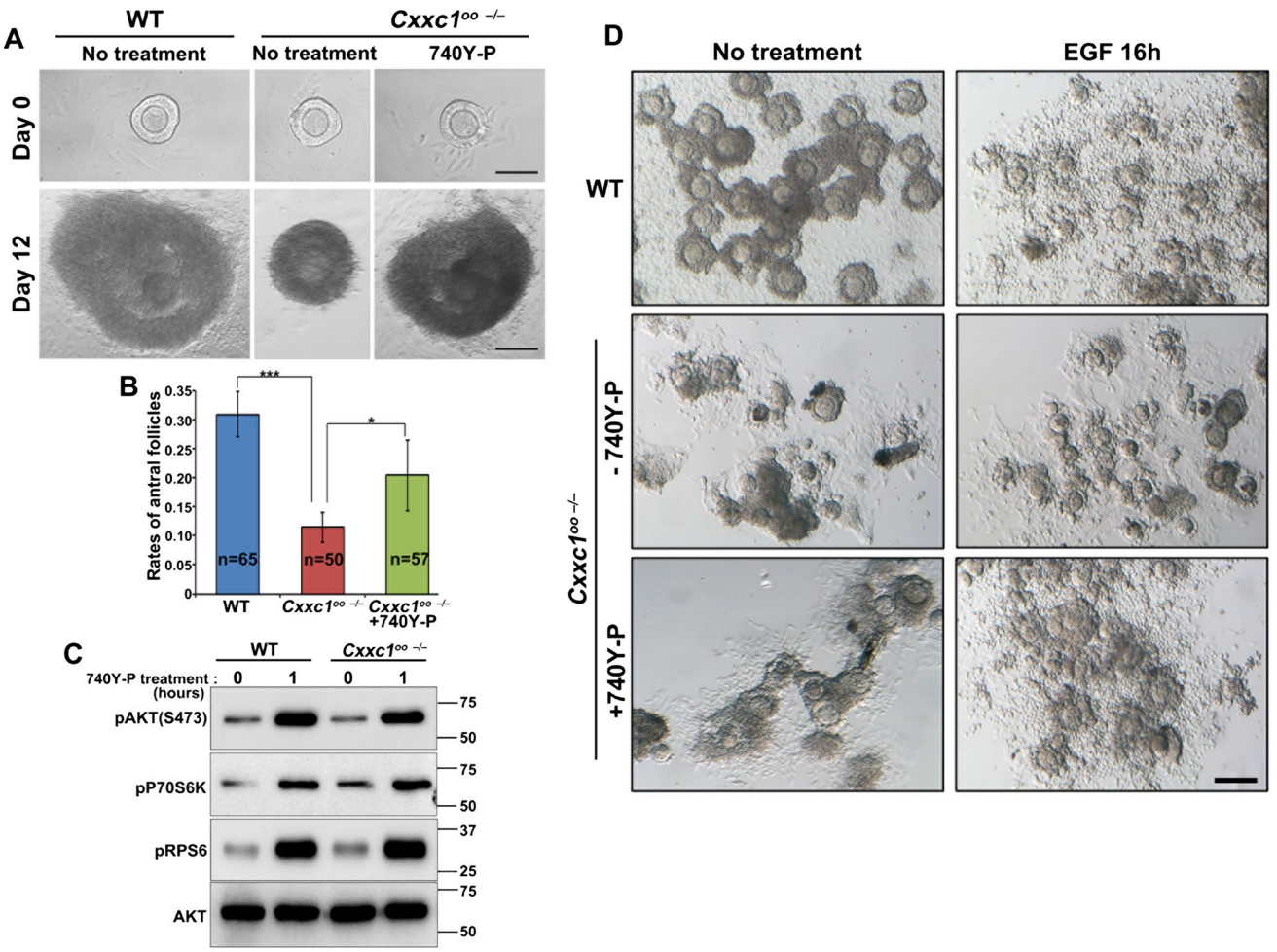

Fig. 5 Rescuing effect of the PI3K activator 740Y-P on cultured *Cxxc1*$^{oo-/-}$ follicles. **a** Representative images of secondary follicles isolated from WT and *Cxxc1*$^{oo-/-}$ ovaries and the same follicle at 12 days after culture with or without adding the PI3K activator 740Y-P. Scale bars 100 μm. **b** Rates of secondary follicles that developed to the antral stage after 12 days' culture. **c** Western blot analysis of PI3K pathway components in cultured GCs before and after 740Y-P (100 μg/ml) treatment for 1 h. Total AKT was blotted as a loading control. **d** COCs isolated from WT and *Cxxc1*$^{oo-/-}$ follicles (with or without 740Y-P treatment) were further cultured in medium with or without adding 100 ng/ml EGF for 16 h before being imaged. Scale bar 150 μm

Some studies have shown that transcription factor FOXO1 is highly expressed in growing follicles and is a negative regulator of steroidogenesis [18, 26, 27]. LH or hCG induces degradation of FOXO1 before ovulation and stimulates steroidogenesis and terminal differentiation of GCs [27]. We found that FOXO1 expression remained high in *Cxxc1*$^{oo-/-}$ ovaries, even after hCG treatment (Fig. 6i), indicating that GC differentiation was impaired after the *Cxxc1* deletion in oocytes. This phenomenon was indeed associated with a lower serum progesterone level in hCG-treated *Cxxc1*$^{oo-/-}$ mice than that in control mice (Fig. 6j). Because the CFP1 protein is deleted only in oocytes (not in mural granulosa or cumulus cells), these results that CFP1 in oocytes was required for ovulation in a cell-nonautonomous manner.

Ovulation-stimulating signals were compromised in granulosa and cumulus cells of *Cxxc1*$^{oo-/-}$ ovaries

In the previous studies, we have shown that the preovulatory LH surge induces transient activation of extracellular signal regulated kinases 1 and -2 (ERK1 and 2) in granulosa and cumulus cells, and that ERK1 and -2 activities are indispensable for LH target gene expression and for ovulation [15]. Thus, we determined protein levels of phosphorylated and activated ERK1 and -2 and their target genes in the GCs of *Cxxc1*$^{oo-/-}$ mice by immunofluorescent staining, western blot, and/or qRT-PCR. These results revealed that ERK1 and -2 phosphorylation remarkably decreased in the granulosa and cumulus cells of *Cxxc1*$^{oo-/-}$ mice at 2 h after hCG injection (Fig. 7a, b). The LH downstream genes—that are

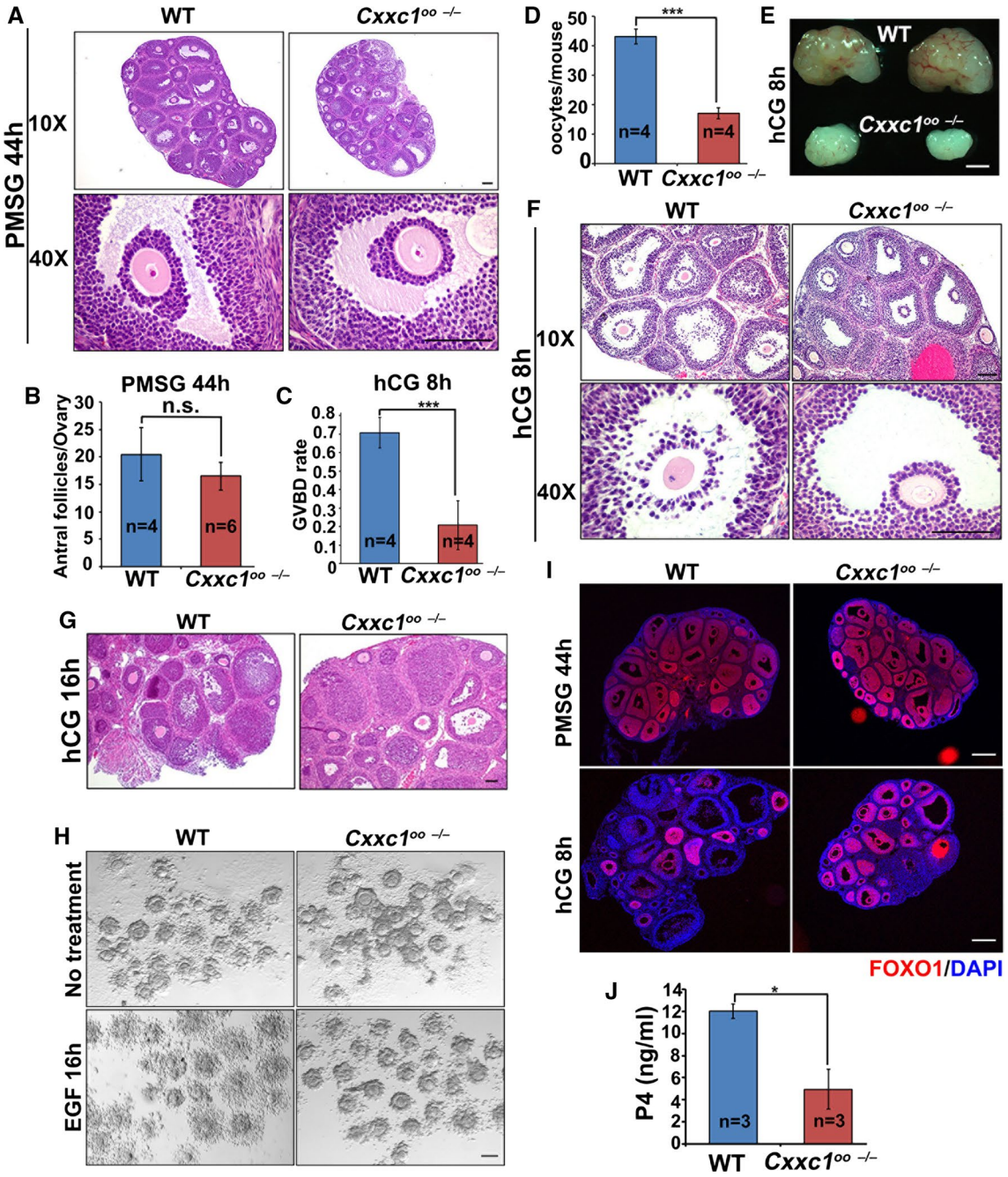

Fig. 6 The impact of oocyte-specific *Cxxc1* deletion on ovulation. **a** H&E staining results showing ovarian histology of 3-week-old WT and *Cxxc1*$^{oo-/-}$ mice 44 h after PMSG priming. Scale bar 100 μm. **b** Antral follicle counts of 3-week-old WT and *Cxxc1*$^{oo-/-}$ ovaries after PMSG priming for 44 h. The numbers of ovaries used for each genotype (*n*) are indicated. Error bars: SEM; *n.s.* nonsignificant. **c** In vivo GVBD rates in antral follicles of 3-week-old WT and *Cxxc1*$^{oo-/-}$ mice at 8 h after hCG injection. Four females of each genotype (*n*) were used in this experiment. Error bars: SEM. $***P<0.001$ according to two-tailed Student's *t* test. **d** Numbers of oocytes ovulated in 3-week-old WT and *Cxxc1*$^{oo-/-}$ mice at 16 h after hCG injection. Four females of each genotype (*n*) were employed in this experiment. Error bars: SEM. $***P<0.001$ according to two-tailed Student's *t* test. **e** Images of ovaries of 3-week-old WT and *Cxxc1*$^{oo-/-}$ mice at 8 h after hCG injection. Scale bar 500 μm. **f** H&E staining results showing ovarian histology of 3-week-old WT and *Cxxc1*$^{oo-/-}$ mice at 8 h after hCG injection. Scale bar 100 μm. **g** H&E staining results showing ovarian histology of 3-week-old WT and *Cxxc1*$^{oo-/-}$ mice at 16 h after hCG injection. Scale bar 100 μm. **h** COC (collected from 4-week-old WT and *Cxxc1*$^{oo-/-}$ mice) expansion induced by EGF at 16 h of culturing. Scale bar 100 μm. **i** Immunofluorescence assay results showing the FOXO1 expression in GCs of WT and *Cxxc1*$^{oo-/-}$ ovaries after PMSG (44 h) and hCG injection (8 h). Scale bar 100 μm. **j** Serum progesterone (P4) concentrations of WT and *Cxxc1*$^{oo-/-}$ mice at 8 h after hCG injection. Four females of each genotype (*n*) were used in this experiment. Error bars: SEM; $0.01<*P<0.05$ according to two-tailed Student's *t* test

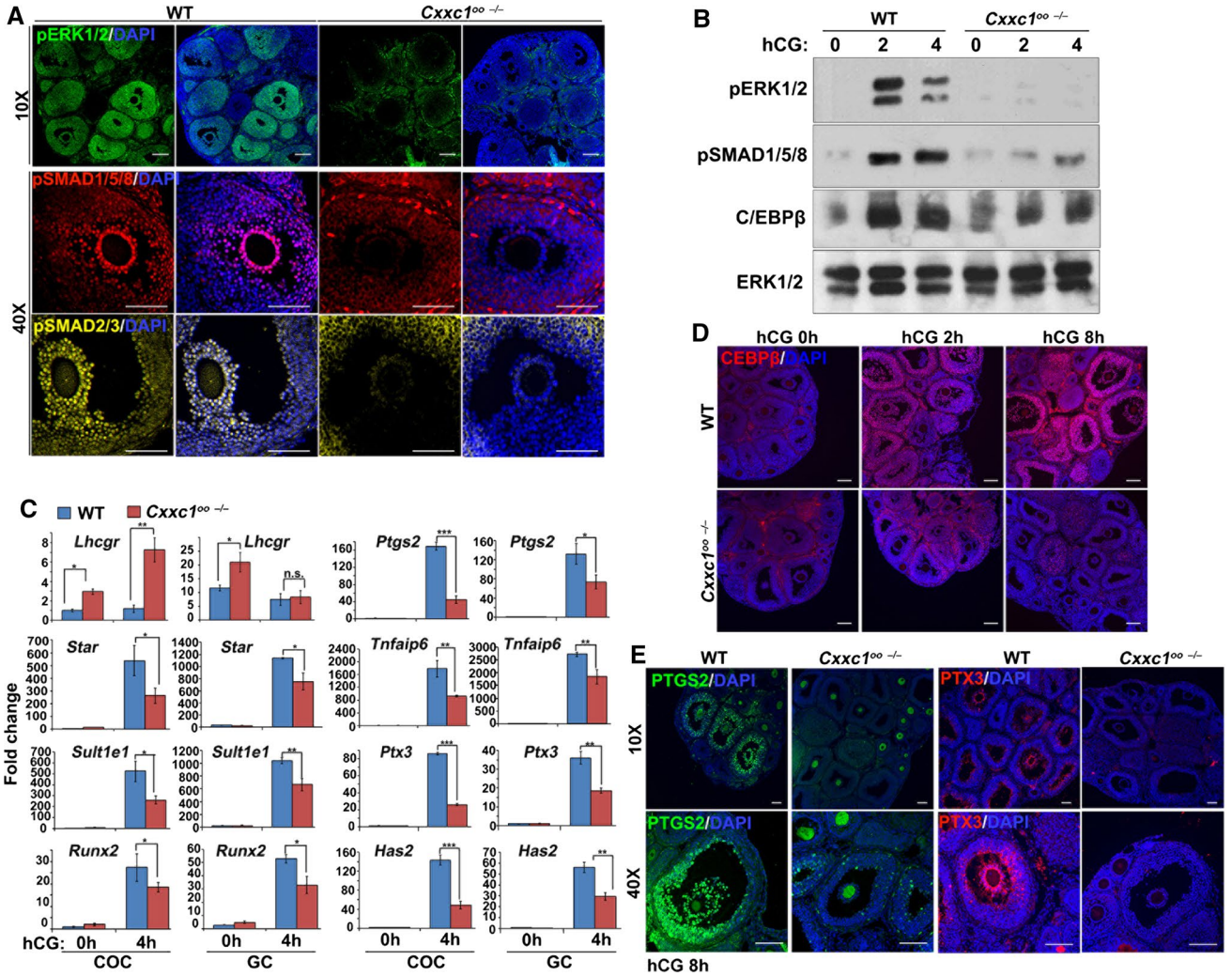

Fig. 7 Detection of ovulation-related signaling events in the ovaries of WT and *Cxxc1*$^{oo-/-}$ mice. **a** Immunofluorescence assay results for phosphorylated ERK1 and -2, SMAD2 and -3, and SMAD1, -5, and -8 in the ovaries of WT and *Cxxc1*$^{oo-/-}$ mice at 2 h after hCG injection. Scale bar 100 μm. **b** Western blot results showing levels of phosphorylated ERK1/-2, SMAD1/5/8, and CEBPβ in the ovaries of WT and *Cxxc1*$^{oo-/-}$ mice before and after hCG injection (0, 2, and 4 h). Total ERK1/2 was blotted as a loading control. Total proteins were extracted from GCs of four ovaries in each group, and 30 μg proteins were loaded per lane; each experiment was repeated for at least three times with the similar results. **c** qRT-PCR results on the expression levels of LH target genes in GCs and COCs isolated from WT and *Cxxc1*$^{oo-/-}$ ovaries (0 and 4 h after hCG injection). Error bars: SEM. $***P<0.001$, $**P<0.01$, and $*P<0.05$ according to two-tailed Student's *t* test. **d** Immunofluorescence assay results showing the expression of transcription factor CEBPβ in the ovaries of WT and *Cxxc1*$^{oo-/-}$ mice before and after hCG injection (2 and 8 h). Scale bar 100 μm. **e** Immunofluorescence assay results showing the expression of PTGS2 and PTX3 in the ovaries of WT and *Cxxc1*$^{oo-/-}$ mice after hCG injection (8 h). Scale bar 100 μm

regulated by ERK1 and -2 and are essential for cumulus expansion (*Ptgs2*, *Ptx3*, *Has2*, and *Tnfaip6*) and for ovarian endocrine functions (*Sult1e1* and *Star*) during ovulation [15]—had significantly lower expression levels in both COCs and GCs of *Cxxc1*$^{oo-/-}$ mice, when compared with those of control mice, at 4 h after hCG injection (Fig. 7c). Notably, in agreement with our observation that CFP1 is required for COCs to maintain their unique gene expression pattern, we noted derepression of LH receptor expression in COCs of *Cxxc1*$^{oo-/-}$ mice (Fig. 7c). Furthermore, CEBPβ (a transcription factor regulated by ERK1 and 2), which is crucial for ovulation [14], was not effectively induced in the ovaries of *Cxxc1*$^{oo-/-}$ mice after hCG injections (Fig. 7b, d).

Some studies have also shown that oocyte-secreted GDF9 and BMP15 induce phosphorylation and activation of their downstream signaling molecules SMAD2 and -3 and SMAD1, -5, and -8, respectively, in adjacent cumulus cells, and that this signaling pathway is a prerequisite for successful cumulus expansion and ovulation [24, 31, 45]. Because the expression of *Gdf9* and *Bmp15* decreased in *Cxxc1*-null oocytes, the TGF-β signaling between a CFP1-deficient oocyte and its surrounding GCs might be impaired.

As presented in Fig. 7a, pSMAD1, -5, and -8 and pSMAD2 and -3 levels were significantly lower in cumulus cells that surrounded *Cxxc1*-null oocytes when compared with those that surrounded WT oocytes. The decrease of pSMAD1/5/8 levels in GCs of *Cxxc1*$^{oo-/-}$ mice when compared with WT mice was also confirmed by western blot (Fig. 7b). Similarly, the protein expression of oocyte factor (GDF9, BMP15, and FGF8)-regulated, ovulation-related genes in cumulus cells, including prostaglandin synthase 2 (PTGS2) and pentraxin-3 (PTX3), decreased in the preovulatory follicles of *Cxxc1*$^{oo-/-}$ mice (Fig. 7e). This result is consistent with the qRT-PCR data in Fig. 7c.

We also checked the mRNA expression of genes coding for EGF-like paracrine factors (*Areg*, *Ereg*, and *Btc*) in granulosa and cumulus cells. These three factors are intrafollicular mediators of LH actions, and are known to be essential for ovulation [36]. Although the mRNA level of *Btc* was lower in granulosa and cumulus cells of *Cxxc1*$^{oo-/-}$ mice after hCG injection, mRNA levels of *Areg* and *Ereg* were not significantly affected by the *Cxxc1* knockout in oocytes (Fig. 8a). Nor was the LH-induced expression of transcription factor GATA-binding protein 4 (GATA4) [30] affected in the ovaries of hCG-treated *Cxxc1*$^{oo-/-}$ mice (Fig. 8b). These results indicated that the *Cxxc1* knockout in oocytes

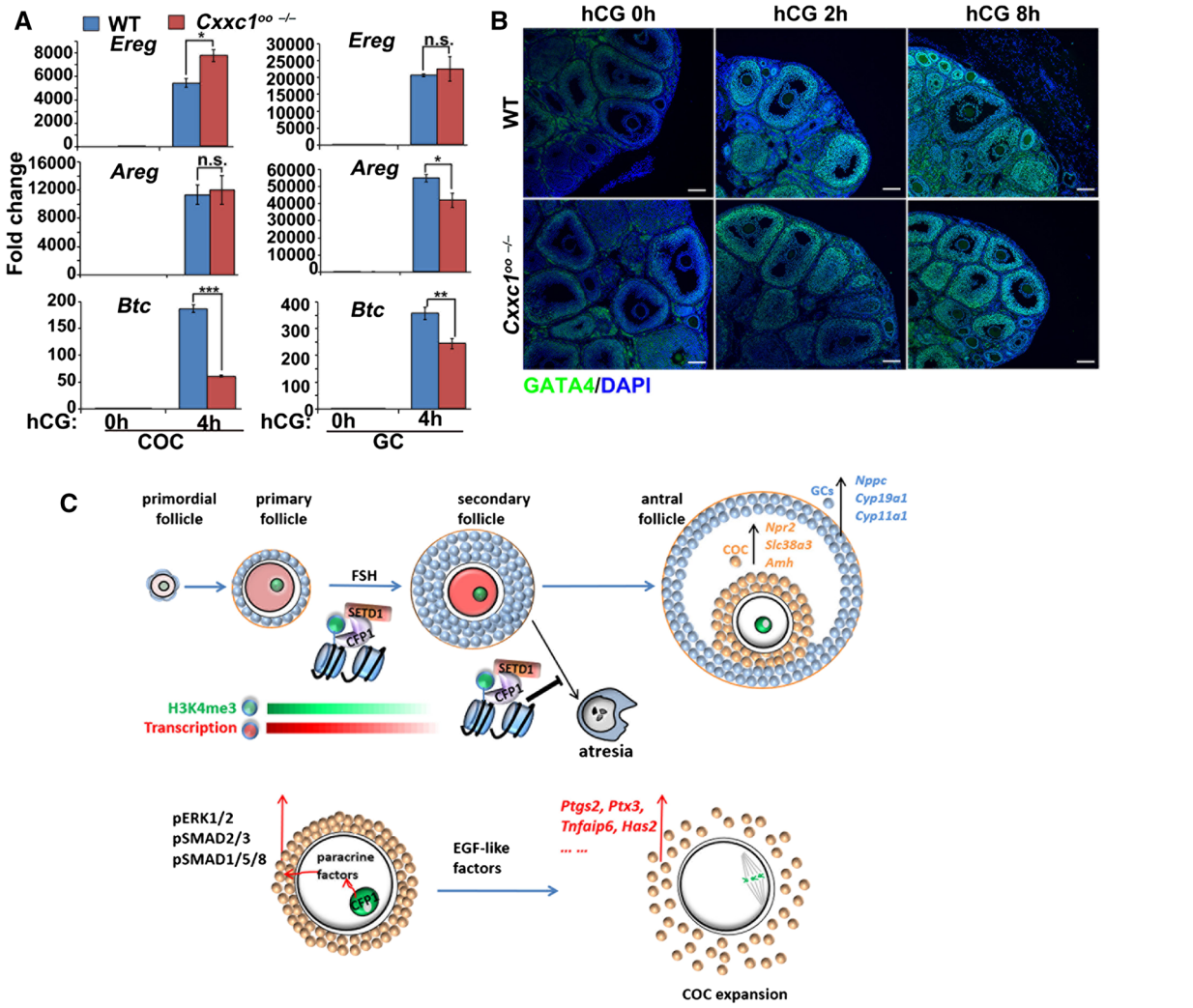

Fig. 8 Expression of EGF-like factors and GATA4 in the ovaries of WT and *Cxxc1*$^{oo-/-}$ mice. **a** qRT-PCR results on the mRNA expression of three EGF-like factors (*Areg*, *Ereg*, and *Btc*) in GCs and COCs isolated from WT and *Cxxc1*$^{oo-/-}$ ovaries (0 and 4 h after hCG injection). Error bars: SEM. $^{**}P<0.01$ and $^{*}P<0.05$ according to two-tailed Student's *t* test; n.s.: nonsignificant. **b** Immunofluorescence assay results showing expression of GATA4 in the ovaries of WT and *Cxxc1*$^{oo-/-}$ mice before and after hCG injection (2 and 8 h). Scale bar 100 μm. **c** A diagram showing functions of CFP1 in mouse oocytes of growing and preovulatory follicles. Accompanied by FSH stimulation, CFP1-SETD1-mediated H3K4 trimethylation in oocytes facilitates the survival of growing follicles and the transition from the secondary to antral follicle stage. In fully grown mouse oocytes of preovulatory follicles, CFP1 is required for oocyte expression of the cumulus expansion-enabling factors, which activate ovulation signaling pathways in the surrounding cumulus cells and maintain COC responsiveness to the ovulation signal triggered by LH

impaired the expression of only a subset of LH-regulated ovulation-related genes in granulosa and cumulus cells.

Discussion

In this study, we identified CFP1 in oocytes as a key regulator of ovarian functions, particularly follicle development and ovulation, as summarized in Fig. 7c. The H3K4me3 level was low in growing oocytes but high in fully grown oocytes, indicating that H3K4me3 is a marker of epigenetic maturation. Defective H3K4 trimethylation in growing oocytes under the influence of the *Cxxc1* knockout impaired the responses of GCs to gonadotropin signals, implying that balanced H3 K4 methylation of the oocyte genome not only is essential for maintaining transcription within the oocyte but also determines the developmental fate of the follicles.

Paracrine factors secreted by oocytes have profound effects on follicle growth and development both before and after the LH surge. For example, the absence of oocyte-derived GDF9 results in a failure to progress beyond the early preantral stages of follicle development [10]. A lack of BMP15, another oocyte-secreted protein, impairs cumulus cell differentiation and cumulus expansion [43]. In particular, oocyte-secreted paracrine factors are necessary to enable upregulation of *Has2*, *Ptgs2*, *Ptx3*, and *Tnfaip6* transcripts during cumulus expansion. Each of these transcripts is absolutely required for cumulus expansion, because the phenotype of null mutations in *Ptgs2*, *Ptx3*, or *Tnfaip6* or inhibition of HAS2 activity severely compromises cumulus expansion.

The CFP1 deletion affected the expression of a wide range of maternal genes, regardless of their original expression magnitude [44]. In addition, deletion of the *Mll2* gene, which encodes another histone H3 lysine-4 trimethylase, in mouse oocytes impairs H3K4me3 accumulation and causes an ovulation defect [2]. Therefore, the obvious question is how those two distinct H3K4 methyltransferases split the labor in terms of H3K4me3 induction. Although the oocyte-specific *Mll2* mice have ovulation defects, the expression levels of *Gdf9*, *Bmp15*, and *c-Kit* in oocytes were not affected by *Mll2* KO [2]. In contrast, these genes were downregulated in *Cxxc1* KO oocytes. Therefore, CFP1 might be more important than MLL2 in maintaining expression of these oocyte-derived paracrine factors and the normal communications between oocytes and surrounding granulosa/cumulus cells. Oocyte-specific knockout of murine *Setd1b* also caused a reduction in ovary size, an increase in atretic follicles, and ovulation defects. These phenotypes are comparable with those observed after CFP1 ablation in oocytes [4]. Because CFP1 is part of the complex that recruits SETD1B to chromatin, the overlap in the phenotypes of the knock-outs further strengthened the notion that the SETD1–CFP1 complex in oocyte is required to maintain normal ovarian functions.

Although GCs express many mRNA transcripts and proteins in common, the mural and cumulus cells each express a subset of different transcripts, with markedly different steady-state levels. The cumulus cells surrounding the oocyte are specialized to service the development of the oocyte, and steroidogenesis is the principal role of mural GCs that line the follicle wall [8, 38]. The findings in this report show that *Cxxc1* deletion in mouse oocytes decreases mRNA transcript levels of cumulus markers. In addition, TGF-β signaling is positively involved in cumulus expansion, and upregulation of *Ptx3*, *Ptgs2*, and *Has2* mRNAs was compromised in follicles containing the *Cxxc1*-null oocytes. By contrast, expression of mural GC transcripts increased in cumulus cells of $Cxxc1^{oo-/-}$ ovaries. Thus, without the CFP1-mediated H3K4me3 accumulation, oocytes failed to establish opposing gradients of influence in the follicle toward the pituitary-secreted FSH. Only the oocytes with appropriate H3K4me3 levels are capable of specifying the mural and cumulus GC phenotypes that are pivotal for follicle development and ovulation.

In recent years, the features and establishment of epigenetic modifications in developing oocytes were extensively studied. Nonetheless, the potential involvement of these epigenetic events in the regulation of ovarian function via cell-nonautonomous mechanisms has not been assessed. In the ovaries of $Cxxc1^{oo-/-}$ mice, the primordial follicle pool is intact, but awakened follicles have low efficiency of development into antral follicles. Instead, they have a higher-than-normal rate of becoming atretic. This phenomenon is most likely due to the lack of PI3K signaling activity in growing follicles. It has been recognized that oocytes coordinate their own survival, GC proliferation, and follicle growth by secreting local signaling molecules and communicate with GCs through gap junctions. KIT and KIT ligand (KITL) have well-documented functions in the proliferation, migration, and differentiation of ovarian follicle cells, primarily by activating the PI3K signaling pathway [19]. KIT is expressed on the primordial oocyte membrane, while KITL is produced by granulosa cells. Therefore, the significant decrease of c-Kit expression in *Cxxc1*-null oocytes might be a major reason for the weakened AKT activity in the surrounding GCs. Consequently, the compromised AKT activity led to the increase of FOXO1 protein level and the high apoptosis rate of GCs. Our results also indicate that the expression of *Gja4*, which encodes oocyte-specific gap junction protein connexin-37 [37], is low in *Cxxc1*-null oocytes. Recently, small molecules that modulate the PI3K pathway have been used for treating the ovarian tissues of human patients with primary ovarian insufficiency for assisted reproduction purposes [22, 41]. On the other hand, it has been unclear

whether CFP1 function and H3K4me3 accumulation are also stimulated in oocytes alone with follicle awakening. Our observations in this novel mouse model suggest that the key role of CFP1 in oocytes of growing follicles should be considered when using these new drugs in clinical practice.

FSH supports follicle growth beyond the early antral stage [9]. In the current study, we provide evidence that depletion of *Cxxc1* impairs the physiological effect of FSH on follicle growth. Thus, we hypothesize that in WT mice, CFP1 together with SETD1 histone methyltransferase promotes accumulation of H3K4me3 in oocytes of growing follicles, thereby increasing the secretion of oocyte-derived paracrine factors as well as the communication between oocytes and cumulus cells and leading to increased follicular responses to gonadotropins (Fig. 8c). This positive feedback loop may potentially perform a key function in follicle selection during each estrous cycle.

Materials and methods

Animals

Mice were maintained in a controlled environment of 20–22 °C, with a 12 h/12 h light/dark cycle, 50–70% humidity, and food and water provided ad libitum. All mice used were handled according to the Animal Research Committee guidelines of Zhejiang University. *Cxxc1*$^{fl/fl}$ mouse strain has been engineered and described previously [7]. They were bred over the *Gdf9-Cre* transgenic mice, which allow CRE-mediated recombination specifically in the oocytes at the primordial follicle stage [21]. All mice have a C57BL/6J genetic background.

Superovulation

To study ovarian responses to exogenous gonadotropins, female mice at postnatal day (PD) 23 were analyzed to avoid the complexity of ovarian functions associated with estrous cycles and endogenous surges of gonadotropins. Immature mice were injected intraperitoneally with 5 IU PMSG (pregnant mare serum gonadotropin; Calbiochem) to stimulate preovulatory follicle development followed 48 h later with 5 IU hCG (human chorionic gonadotropin, American Pharmaceutical Partners, Schaumburg, IL, USA) to stimulate ovulation.

In vitro COC expansion assay

Fully grown, non-expanded COCs were collected from ovaries of PMSG-primed immature mice. COCs (~30) were plated in 100 µl of defined COC medium (MEM w/ES, 25 mM HEPES, 0.25 mM sodium pyruvate, 3 mM L-glutamine, 1 mg/ml BSA, 100 U/mL penicillin, and 100 µg/ml streptomycin) with 1% FBS under the cover of mineral oil and treated with EGF (100 ng/ml) or FSH (500 nM). Expansion status was evaluated by microscopic examination after overnight culture.

Histological analysis

Ovaries were collected and fixed in formalin overnight, processed, and embedded in paraffin using standard protocols. IHC was performed using standard protocols. For immunofluorescence, sections or cells were sequentially probed with primary antibodies as indicated in Results and Alexa Fluor 594- or 488-conjugated secondary antibodies (Molecular Probes). Slides were mounted using VectaShield with 4′,6-diamidino-2-phenylindole (DAPI, Vector Laboratories). Digital images were acquired using an epifluorescence microscope (Nikon Eclipse 80i) with 4–100× objectives. Semi-quantitative analysis of the fluorescence signals was conducted using the NIH Image analysis program ImageJ. The relative H3K4me3 and pS2 levels were quantified by comparing the Alexa Fluor 594 or 488 fluorescence intensities with the intensity of DAPI staining within the same oocyte. The blue channel of DAPI staining was not presented in the original figure due to the space limitation. The antibodies used are listed in Supplementary Table 1.

Follicle counts

Ovaries were serially sectioned at 5 µm and stained with hematoxylin and eosine (H&E). Numbers of follicles were determined by recording the numbers of oocyte nuclei on all sections. These criteria were used to determine the follicle stages: primordial follicles, small oocytes surrounded by a single layer of flat granulosa cells; primary follicles, middle sized oocytes surrounded by a single layer of cubical granulosa cells; secondary follicles, large oocytes surrounded by more than two layers of granulosa cells; antral follicles and presence of follicle cavity.

TUNEL assay

TUNEL assays were performed on 10% formalin-fixed paraffin-embedded sections using the ApopTag Plus Peroxidase In Situ Apoptosis Detection Kit (Serologicals Corporation, Norcross, GA, USA) according to the manufacturer's instructions.

Hormone-level assays

Mice were anesthetized and blood was collected by cardiac puncture. Serum and blood cells were separated by centrifugation. Serum hormone levels were determined by

Di'an Medical Diagnostics Limited Corporation (Hangzhou, China).

Western blot

Ovaries were lysed in 2-mercaptoethanol containing loading buffer and heated at 95 °C for 5 min. SDS-PAGE and immunoblots were performed following the standard procedures using a Mini-PROTEAN Tetra Cell System (Bio-Rad, Hercules, CA, USA). The antibodies used are listed in Supplementary Table 1.

Quantitative RT-PCR

Total RNA was extracted from oocytes using the RNeasy Mini kit (Qiagen) according to the manufacturer's instruction, followed by reverse transcription (RT) using Superscript RT kit (Bio-Rad). Quantitative RT-PCR was performed using a Power SYBR Green PCR Master Mix (Applied Biosystems, Life technologies) with ABI 7500 Real-Time PCR system (Applied Biosystems) using primers listed in Supplementary Table 2. For each indicated gene, the relative transcript level of the control sample (left-hand bar of each graph) was set as 1. The relative transcript levels of other samples were compared to the control, and the fold-changes shown in the graph. For each experiment, qPCR reactions were done in triplicate.

ChIP-qPCR

For ChIP-qPCR, 300 oocytes were used per reaction. The procedure of ULI-NChIP was carried out as previously described [46]. 1 µg of histone H3K4me3 antibody (Cell Signaling Technology, catalog no.9727) was used for each immunoprecipitation reaction. Then, we used 3 ng/µl DNA obtained from the ChIP experiments and 10 ng/µl input DNA for ChIP-qPCR analysis. The primers used in the qPCR experiment are listed in Supplementary Table 2.

Statistical analysis

The experiments were randomized and were performed with blinding to the conditions of the experiments. No statistical method was used to predetermine sample size. Results are given as mean ± SEM. Each experiment included at least three independent samples and was repeated at least two times. Results for two experimental groups were compared by two-tailed unpaired Student's *t* tests. Statistically significant values of $P < 0.05$, $P < 0.01$, and $P < 0.001$ are indicated by asterisks (*), (**), and (***), respectively.

Publicly available data

Raw sequencing reads were obtained from Gene Expression Omnibus and processed with the parameters detailed below: *Cxxc1*-null oocytes (GSE85019).

Acknowledgements This study is funded by the National Key Research and Developmental Program of China (2017YFC1001500, 2016YFC1000600), National Natural Science Foundation of China (31528016, 31371449, 31671558), and The Key Research and Development Program of Zhejiang Province (2017C03022).

Compliance with ethical standards

Conflict of interest No competing interests declared.

References

1. Adhikari D, Liu K (2009) Molecular mechanisms underlying the activation of mammalian primordial follicles. Endocr Rev 30:438–464
2. Andreu-Vieyra CV, Chen R, Agno JE, Glaser S, Anastassiadis K, Stewart AF, Matzuk MM (2010) MLL2 is required in oocytes for bulk histone 3 lysine 4 trimethylation and transcriptional silencing. PLoS Biol 2010:8
3. Bledau AS, Schmidt K, Neumann K, Hill U, Ciotta G, Gupta A, Torres DC, Fu J, Kranz A, Stewart AF, Anastassiadis K (2014) The H3K4 methyltransferase Setd1a is first required at the epiblast stage, whereas Setd1b becomes essential after gastrulation. Development 141:1022–1035
4. Brici D, Zhang Q, Reinhardt S, Dahl A, Hartmann H, Schmidt K, Goveas N, Huang J, Gahurova L, Kelsey G, Anastassiadis K, Stewart AF, Kranz A (2017) Setd1b, encoding a histone 3 lysine 4 methyltransferase, is a maternal effect gene required for the oogenic gene expression program. Development 144:2606–2617
5. Brown C, LaRocca J, Pietruska J, Ota M, Anderson L, Smith SD, Weston P, Rasoulpour T, Hixon ML (2010) Subfertility caused by altered follicular development and oocyte growth in female mice lacking PKB alpha/Akt1. Biol Reprod 82:246–256
6. Brown DA, Di Cerbo V, Feldmann A, Ahn J, Ito S, Blackledge NP, Nakayama M, McClellan M, Dimitrova E, Turberfield AH, Long HK, King HW, Kriaucionis S, Schermelleh L, Kutateladze TG, Koseki H, Klose RJ (2017) The SET1 complex selects actively transcribed target genes via multivalent interaction with CpG island chromatin. Cell Rep 20:2313–2327
7. Cao W, Guo J, Wen X, Miao L, Lin F, Xu G, Ma R, Yin S, Hui Z, Chen T, Guo S, Chen W, Huang Y, Liu Y, Wang J, Wei L, Wang L (2016) CXXC finger protein 1 is critical for T-cell intrathymic development through regulating H3K4 trimethylation. Nat Commun 7:11687
8. Diaz FJ, Wigglesworth K, Eppig JJ (2007) Oocytes determine cumulus cell lineage in mouse ovarian follicles. J Cell Sci 120:1330–1340
9. Dierich A, Sairam MR, Monaco L, Fimia GM, Gansmuller A, LeMeur M, Sassone-Corsi P (1998) Impairing follicle-stimulating hormone (FSH) signaling in vivo: targeted disruption of the FSH receptor leads to aberrant gametogenesis and hormonal imbalance. Proc Natl Acad Sci USA 95:13612–13617

10. Dong J, Albertini DF, Nishimori K, Kumar TR, Lu N, Matzuk MM (1996) Growth differentiation factor-9 is required during early ovarian folliculogenesis. Nature 383:531–535
11. Eppig JJ (2001) Oocyte control of ovarian follicular development and function in mammals. Reproduction 122:829–838
12. Eppig JJ, Wigglesworth K, Chesnel F (1993) Secretion of cumulus expansion enabling factor by mouse oocytes: relationship to oocyte growth and competence to resume meiosis. Dev Biol 158:400–409
13. Fan HY, Liu Z, Cahill N, Richards JS (2008) Targeted disruption of Pten in ovarian granulosa cells enhances ovulation and extends the life span of luteal cells. Mol Endocrinol 22:2128–2140
14. Fan HY, Liu Z, Johnson PF, Richards JS (2011) CCAAT/enhancer-binding proteins (C/EBP)-alpha and -beta are essential for ovulation, luteinization, and the expression of key target genes. Mol Endocrinol 25:253–268
15. Fan HY, Liu Z, Shimada M, Sterneck E, Johnson PF, Hedrick SM, Richards JS (2009) MAPK3/1 (ERK1/2) in ovarian granulosa cells are essential for female fertility. Science 324:938–941
16. Gu L, Wang Q, Sun QY (2010) Histone modifications during mammalian oocyte maturation: dynamics, regulation and functions. Cell Cycle 9:1942–1950
17. Hanna CW, Taudt A, Huang J, Gahurova L, Kranz A, Andrews S, Dean W, Stewart AF, Colome-Tatche M, Kelsey G (2018) MLL2 conveys transcription-independent H3K4 trimethylation in oocytes. Nat Struct Mol Biol 25:73–82
18. Herndon MK, Law NC, Donaubauer EM, Kyriss B, Hunzicker-Dunn M (2016) Forkhead box O member FOXO1 regulates the majority of follicle-stimulating hormone responsive genes in ovarian granulosa cells. Mol Cell Endocrinol 434:116–126
19. John GB, Shidler MJ, Besmer P, Castrillon DH (2009) Kit signaling via PI3K promotes ovarian follicle maturation but is dispensable for primordial follicle activation. Dev Biol 331:292–299
20. Knight PG, Glister C (2006) TGF-beta superfamily members and ovarian follicle development. Reproduction 132:191–206
21. Lan ZJ, Xu X, Cooney AJ (2004) Differential oocyte-specific expression of Cre recombinase activity in GDF-9-iCre, Zp3cre, and Msx2Cre transgenic mice. Biol Reprod 71:1469–1474
22. Li J, Kawamura K, Cheng Y, Liu S, Klein C, Liu S, Duan EK, Hsueh AJ (2010) Activation of dormant ovarian follicles to generate mature eggs. Proc Natl Acad Sci USA 107:10280–10284
23. Li Q, He H, Zhang YL, Li XM, Guo X, Huo R, Bi Y, Li J, Fan HY, Sha J (2013) Phosphoinositide 3-kinase p110delta mediates estrogen- and FSH-stimulated ovarian follicle growth. Mol Endocrinol 27:1468–1482
24. Li Q, Pangas SA, Jorgez CJ, Graff JM, Weinstein M, Matzuk MM (2008) Redundant roles of SMAD2 and SMAD3 in ovarian granulosa cells in vivo. Mol Cell Biol 28:7001–7011
25. Liu X, Wang C, Liu W, Li J, Li C, Kou X, Chen J, Zhao Y, Gao H, Wang H, Zhang Y, Gao Y, Gao S (2016) Distinct features of H3K4me3 and H3 K27me3 chromatin domains in pre-implantation embryos. Nature 537:558–562
26. Liu Z, Ren YA, Pangas SA, Adams J, Zhou W, Castrillon DH, Wilhelm D, Richards JS (2015) FOXO1/3 and PTEN depletion in granulosa cells promotes ovarian granulosa cell tumor development. Mol Endocrinol 29:1006–1024
27. Liu Z, Rudd MD, Hernandez-Gonzalez I, Gonzalez-Robayna I, Fan HY, Zeleznik AJ, Richards JS (2009) FSH and FOXO1 regulate genes in the sterol/steroid and lipid biosynthetic pathways in granulosa cells. Mol Endocrinol 23:649–661
28. McGee EA, Hsueh AJ (2000) Initial and cyclic recruitment of ovarian follicles. Endocr Rev 21:200–214
29. Otsuka F, Yao Z, Lee T, Yamamoto S, Erickson GF, Shimasaki S (2000) Bone morphogenetic protein-15. Identification of target cells and biological functions. J Biol Chem 275:39523–39528
30. Padua MB, Fox SC, Jiang T, Morse DA, Tevosian SG (2014) Simultaneous gene deletion of gata4 and gata6 leads to early disruption of follicular development and germ cell loss in the murine ovary. Biol Reprod 91:24
31. Pangas SA, Li X, Umans L, Zwijsen A, Huylebroeck D, Gutierrez C, Wang D, Martin JF, Jamin SP, Behringer RR, Robertson EJ, Matzuk MM (2008) Conditional deletion of Smad1 and Smad5 in somatic cells of male and female gonads leads to metastatic tumor development in mice. Mol Cell Biol 28:248–257
32. Reddy P, Adhikari D, Zheng W, Liang S, Hamalainen T, Tohonen V, Ogawa W, Noda T, Volarevic S, Huhtaniemi I, Liu K (2009) PDK1 signaling in oocytes controls reproductive aging and lifespan by manipulating the survival of primordial follicles. Hum Mol Genet 18:2813–2824
33. Richard S, Baltz JM (2014) Prophase I arrest of mouse oocytes mediated by natriuretic peptide precursor C requires GJA1 (connexin-43) and GJA4 (connexin-37) gap junctions in the antral follicle and cumulus-oocyte complex. Biol Reprod 90:137
34. Sha QQ, Dai XX, Jiang JC, Yu C, Jiang Y, Liu J, Ou XH, Zhang SY, Fan HY (2018) CFP1 coordinates histone H3 lysine-4 trimethylation and meiotic cell cycle progression in mouse oocytes. Nat Commun 9:3477
35. Shilatifard A (2012) The COMPASS family of histone H3K4 methylases: mechanisms of regulation in development and disease pathogenesis. Annu Rev Biochem 81:65–95
36. Shimada M, Hernandez-Gonzalez I, Gonzalez-Robayna I, Richards JS (2006) Paracrine and autocrine regulation of epidermal growth factor-like factors in cumulus oocyte complexes and granulosa cells: key roles for prostaglandin synthase 2 and progesterone receptor. Mol Endocrinol 20:1352–1365
37. Simon AM, Goodenough DA, Li E, Paul DL (1997) Female infertility in mice lacking connexin 37. Nature 385:525–529
38. Su YQ, Sugiura K, Wigglesworth K, O'Brien MJ, Affourtit JP, Pangas SA, Matzuk MM, Eppig JJ (2008) Oocyte regulation of metabolic cooperativity between mouse cumulus cells and oocytes: BMP15 and GDF9 control cholesterol biosynthesis in cumulus cells. Development 135:111–121
39. Su YQ, Wu X, O'Brien MJ, Pendola FL, Denegre JN, Matzuk MM, Eppig JJ (2004) Synergistic roles of BMP15 and GDF9 in the development and function of the oocyte-cumulus cell complex in mice: genetic evidence for an oocyte-granulosa cell regulatory loop. Dev Biol 276:64–73
40. Sugiura K, Su YQ, Diaz FJ, Pangas SA, Sharma S, Wigglesworth K, O'Brien MJ, Matzuk MM, Shimasaki S, Eppig JJ (2007) Oocyte-derived BMP15 and FGFs cooperate to promote glycolysis in cumulus cells. Development 134:2593–2603
41. Sun X, Su Y, He Y, Zhang J, Liu W, Zhang H, Hou Z, Liu J, Li J (2015) New strategy for in vitro activation of primordial follicles with mTOR and PI3K stimulators. Cell Cycle 14:721–731
42. Vanderhyden BC, Caron PJ, Buccione R, Eppig JJ (1990) Developmental pattern of the secretion of cumulus expansion–enabling factor by mouse oocytes and the role of oocytes in promoting granulosa cell differentiation. Dev Biol 140:307–317
43. Yan C, Wang P, DeMayo J, DeMayo FJ, Elvin JA, Carino C, Prasad SV, Skinner SS, Dunbar BS, Dube JL, Celeste AJ, Matzuk MM (2001) Synergistic roles of bone morphogenetic protein 15 and growth differentiation factor 9 in ovarian function. Mol Endocrinol 15:854–866
44. Yu C, Fan X, Sha QQ, Wang HH, Li BT, Dai XX, Shen L, Liu J, Wang L, Liu K, Tang F, Fan HY (2017) CFP1 regulates histone H3K4 trimethylation and developmental potential in mouse oocytes. Cell Rep 20:1161–1172
45. Yu C, Zhang YL, Fan HY (2013) Selective Smad4 knockout in ovarian preovulatory follicles results in multiple defects in ovulation. Mol Endocrinol 27:966–978

46. Zhang B, Zheng H, Huang B, Li W, Xiang Y, Peng X, Ming J, Wu X, Zhang Y, Xu Q, Liu W, Kou X, Zhao Y, He W, Li C, Chen B, Li Y, Wang Q, Ma J, Yin Q, Kee K, Meng A, Gao S, Xu F, Na J, Xie W (2016) Allelic reprogramming of the histone modification H3K4me3 in early mammalian development. Nature 537:553–557
47. Zhang M, Su YQ, Sugiura K, Xia G, Eppig JJ (2010) Granulosa cell ligand NPPC and its receptor NPR2 maintain meiotic arrest in mouse oocytes. Science 330:366–369
48. Zheng H, Huang B, Zhang B, Xiang Y, Du Z, Xu Q, Li Y, Wang Q, Ma J, Peng X, Xu F, Xie W (2016) Resetting epigenetic memory by reprogramming of histone modifications in mammals. Mol Cell 63:1066–1079